01998 Springer-Verlag New York, Inc.
The Productivity & Sustainability of Southern Forest Ecosystems in a Changing Environment
Edited by Mickler and Fox

38. Detecting and Predicting Climatic Variation from Old-Growth Baldcypress

Gregory A. Reams and Paul C. Van Deusen

Tree-ring data can extend back in time for thousands of years allowing researchers to reconstruct certain environmental factors that have left an imprint or signal in the tree-ring record. Typically, these factors include reconstructions of annual precipitation or temperature for months or seasons to which a particular tree species is sensitive. Over the last several decades, scientists have used tree-ring records in novel ways to investigate the timing and extent of such natural phenomena as volcanoes (Baillie and Munro, 1988), earthquakes (Sheppard and Jacoby, 1987), El Niño/southern oscillation (Stahle and Cleaveland, 1993), fire (Swetnam 1993), carbon dioxide (CO,) (Graybill and Idso, 1993), and synchronous landscape-level disturbances (Reams and Van Deusen, 1993) by recognizing the possibility that various signals may be recorded in the growth record of trees, depending on microsite characteristics, geographic location, and disturbance history (Fritts 1976).

Climate reconstruction from tree-ring data involves establishing a relationship between the tree-ring variable(s) and some measure of climate. The uniformitarian assumption (Fritts, 1976) is then called upon to allow for using this established relationship to reconstruct the climate variable during the period before climate measurements were available. Weather stations in the United States were rarely in place prior to approximately 1860, but many living trees provide data for centuries before that time. Thus, the motivation to use tree-ring derived variables to reconstruct climate is clear.

The usual procedure involves fitting a regression equation that uses climate as the dependent variable and tree-ring data as the independent variable over the period when climate has been recorded. This calibration equation (Fritts, 1976) is then used to predict the earlier, unknown climate data. Stahle and Cleaveland (1992) provide a recent example of this approach using baldcypress (*Taxodium distichum* (L.) Rich.). An alternative approach has been presented by Graumlich (1993), which uses response-surface methods to simultaneously reconstruct temperature and precipitation variables. However, neither of these studies presented confidence intervals around the reconstructions.

In this chapter, we present a new procedure for climate reconstruction that allows for the incorporation of prior knowledge about the climate variable, and that demonstrates the existence of a hurricane signal in the tree-ring data. The climate reconstruction method is applied to old-growth baldcypress data from Louisiana using the Palmer Drought Severity Index (PDSI) for the month of June. We show that the method is relatively easy to program and produces valid confidence intervals as a byproduct. The actual algorithm involved is the Gibbs sampler (Smith and Gelfand, 1992).

The identification of a hurricane signal in these data addresses the increased concern that climate change caused by increased emissions of greenhouse gases may lead to either intensification or greater frequency of extreme storms (Schmidt and von Storch, 1993). Emanuel (1987) found that, given August mean conditions over the tropical oceans with twice the present atmospheric CO, content, a general circulation model (GCM) predicts a 40 to 50% increase in the destructive potential of hurricanes. Jarrell and Elsberry (1994) suggested that global warming might increase the frequency of tropical cyclones because it would expand the area of oceans with temperatures above the 26 °C threshold required for the formation of tropical cyclones. Baldcypress is a uniquely valuable species for investigating the long-term frequency of hurricanes because baldcypress trees are long-lived, and accumulating evidence indicates they withstand hurricanes better than any other tree species in the southern United States (Putz and Sharitz, 1991; Sheffield and Thompson, 1992).

Baldcypress Habitat

Baldcypress is a deciduous conifer that grows on saturated and seasonally inundated soils of the southeastern and Gulf coastal plains. Inland, baldcypress grows along the many streams of the middle- and upper-coastal plains and northward through the Mississippi Valley. Humid, moist subhumid, and dry subhumid climatic types occur within the range of baldcypress. Baldcypress occurs most frequently on intermittently flooded sites, and therefore drainage may be more important than rainfall in determining site suitability. The growing season within the natural range of baldcypress increases from about 190 days in southern Illinois to nearly year-long in southern Florida.

More than 90% of the natural baldcypress stands are on flat topography or in slight depressions at elevations of less than 30 meters above sea level. Baldcypress sites are characterized by frequent, prolonged flooding. Floodwaters may be 3 meters deep or more and may flow at rates up to 6.5 kilometers per hour or may be stagnant. Normally the species is found on intermittently flooded and very poorly drained Spodosols, Ultisols, Inceptisols, Alfisols, and Entisols. The soil temperature regimes are classified as thermic to hyperthermic.

Cypress swamps and other forested wetlands that receive periodic nutrients subsided from floodwaters probably are some of the world's most productive ecosystems. The annual aboveground production of biomass in a baldcypress forest in Florida is 15,700 kg per hectare (ha). In comparison, terrestrial forest communities in the temperate region often produce 12,300 to 15,000 kg/ha annually. Stillwater forested wetlands do not receive nutrient subsidies from floodwaters, and they have production rates comparable to, or lower than, those of terrestrial forests.

Early estimates of the area of baldcypress forests in Louisiana range from 0.67 to 3.64 million ha (Conner and Toliver, 1990). Baldcypress was cut extensively from 1890 to 1925 when the last virgin stands were depleted. Recent estimates indicate that there are 0.14 million ha left in Louisiana (Conner and Toliver, 1990). Williston et al., (1980) estimates that there are between 1.2 and 2 million ha of cypress forest in the United States, with a total growing-stock volume of 155.7 million m^3. Over one-half of the cypress is in Florida and Louisiana, with Louisiana ranked first in timber quality of cypress. Baldcypress growing-stock increased from 15 million m^3 in 1954 to 4 1 million m^3 in 1984. At present, loblolly pine (*Pinus* ***taeda*** L.) and sweetgum (*Liquidambar styraciflua* L.) are the only species in Louisiana with timber volume greater than baldcypress (Rosson et al., 1988)

Methods

Sample

Old-growth baldcypress trees are scattered individually and within small stands throughout many river basins and estuaries in the southeastern United States. These old-growth remnants exist because the trees were considered uneconomical to harvest either because of defect or location. To locate our study sites and eliminate unnecessary field work, we utilized various remote sensing techniques including satellite imagery, NASA's Stennis Space Center calibrated airborne multispectral scanner (CAMS) data, and aerial photography. We began this study in the early summer of 1992 in the Tangipahoa River basin, Louisiana. During 1993 we expanded site selection to the Pearl River basin, Mississippi, and in 1994 began sampling old-growth baldcypress in the Atchafalaya River basin, Louisiana. The results presented here, however, will be restricted to the tree-ring material sampled from the Tangipahoa River and Pearl River basins.

After identifying candidate old-growth sites from remotely sensed data we visited the sites and collected our data using standard increment core sampling techniques with a few minor modifications that greatly increased the temporal depth of our tree cores. Increment cores were extracted from the base of each tree at heights between 60 and 137 cm aboveground, depending on the soundness of the main stem. In prior studies involving old-growth baldcypress, researchers sampled above the well-known root buttress (Stahle et al., 1985, 1988). Trees in our study site showed little to no buttressing, but exhibited heartrot (and therefore hollowness) that increased with sampling height. The heartrot is caused by a fungus, *Stereum taxodi*, and is prevalent in old-growth baldcypress. The fungus gains entrance in the crown and slowly works downward, frequently destroying heartwood to the base of the tree (Wilhite and Toliver, 1990). We often were able to extract more heartwood and thereby add hundreds of annual ring-widths by sampling as close to ground level as possible. Annual increments of each tree core were measured to within 0.001 mm and cross-dated using graphical and statistical procedures available in DYNACLIM (Van Deusen, 1990).

The main data quality concern in tree-ring studies is that the annual ring-widths be measured accurately and precisely, but even more important is that the ring-width be assigned to the correct calendar year. This process is known as cross-dating and is the cornerstone of dendrochronological studies. In dendrochronology, quality control takes place every time a tree core is measured because after the removal of a long-term trend (i.e., standardization), climate-sensitive tree species have the same standardized growth pattern across trees such that the actual data of any one ring of the pattern is the same among trees (Douglass, 1941). This is possible because similar environmental conditions have limited high frequency fluctuations in radial growth.

Bayesian Climate Model

We will begin by designating the tree-ring variable as y_t and the climate variable as x_t. The subscript indicates year t, in which $t = 1, \ldots, T$ is the period over which the tree-ring data are available. We will assume that the climate data are available over the period $t = t_1, \ldots, T$ with $1 < t_1 < T$. Note that the variable y_t could be ring-width, density or some other derived variable. When convenient, we refer to the entire time series of climate or tree data as X and Y, in which X includes the unknown part of the climate series unless otherwise specified.

Now assume that the probability of x_t given Y is a normal distribution:

$$L(X_t \mid Y) = N(f(Y), q\sigma_t^2) \tag{1a}$$

Basically, f(Y) could be any linear or nonlinear function of the tree data including a function in which y_t is a vector of multiple values from different chronologies or derived variables. We estimate σ_t^2 from the individual tree standardized data for each time period. The q-parameter is estimated from that part of the data in which both X and Y are known as described in the example application section following.

Next, we incorporate the prior information also as a normal distribution for x_t conditional on the rest of the climate data denoted as X_{-t}:

$$p(x_t \mid X_{-t}) = N(g(X_{-t}), p) \tag{1b}$$

The function, $g(X_{-t})$, could be a random walk, an autoregressive model of order r, AR(r), or any function of X_{-t} that sensibly describes the climate time series. The p-parameter is estimated from the known climate series as described later.

Finally, using Bayes rule and well-known results about normal probabilities and priors, we get the posterior distribution (Box and Tiao, 1973) for climate given the tree data:

$$p(x_t \mid X_{-t}, Y) = N(\hat{x}_t, D^{-1}) \tag{1c}$$

in which

$$D = \frac{1}{q\sigma_t^2} + \frac{1}{p} \tag{1d}$$

and

$$\hat{x}_t = \left[\frac{f(y_t)}{q\sigma_t^2} + \frac{g(X_{-t})}{p}\right] D^{-1} \tag{1e}$$

The Gibbs Sampler

A moment's reflection leads to the realization that $\hat{x}_t$ in equation (1 e) can only be evaluated if $\hat{X}_{-t}$ is known. Thus, it is clear that an iterative procedure is called for that can begin with a set of starting values and converge to the optimum solution. This is provided by the Gibbs sampler (Carlin et al., 1992).

The desired solution is provided by $p(X \mid Y)$, which is the posterior distribution of the complete climate data given the tree data. The Gibbs sampler begins with a set of arbitrary starting values $X^0 = (x_1^0, \ldots, x_T^0)$, and then makes successive drawings from the conditional posterior distributions described by (1c) as follows:

$$x_1^1 \text{ from } p(x_1 \mid X_{-1}^0, Y)$$
$$x_2^1 \text{ from } p(x_2 \mid x_1^1, x_3^0, \ldots, x_T^0, Y)$$
$$x_3^1 \text{ from } p(x_3 \mid x_1^1, x_2^1, x_4^0, \ldots, x_T^0, Y)$$
$$\vdots$$
$$x_T^1 \text{ from } p(x_T \mid X_{-T}^1, Y)$$

This completes a cycle that takes X^0 to X^1. It has been proven (Geman and Geman, 1984) that X^K, for suitably large K, can be treated as a random sample from $p(X \mid Y)$, which is the posterior distribution we seek. In the example application to follow, we let K = 1,000 and simultaneously generate 1,000 independent outcomes at each stage of the Gibbs sampler. This makes it easy to compute the mean and variance of the reconstructed series. Simply take the 1000 independent climate reconstructions that were generated after the Kth pass of the Gibbs sampler and average them to compute a mean climate reconstruction, $\hat{X}$. Similarly, the variance for each time, t, is computed from the 1,000 time t reconstructions. We chose 1,000 for both K and the number of independent reconstructions principally because 1,000 seemed more than adequate for both values. However, this did require several hours of computation at a Unix workstation.

Hurricane Signal Detection

We have chosen several methods to illustrate that hurricanes have left their imprint on tree-ring records of baldcypress growing near the Gulf of Mexico which are 1) standardized (high frequency) ring-width series and coincidence of known hurricanes, 2) large deviations or influential data points in a growth-climate model that coincide with known hurricanes, and 3) standardized ring-width variation of old-growth vs second-growth (young) trees.

Over forty hurricanes have made landfall along the coastal area between the Atchafalaya River, Louisiana east to the Mobile River in Alabama since 183 1 (Ludlum, 1963). We first noted evidence that baldcypress may contain a hurricane signal during the initial measurement of our tree-ring material from old-growth baldcypress located in the Tangipahoa River basin, Louisiana. We began to notice that many, but not all, old trees had small ring-widths the year of a hurricane and also the year after a hurricane strike (Figure 38.1). A small ring-width the year after a hurricane is more frequent than the year of the hurricane. Accurate hurricane path information for the study area is available from 1871 to 1986 (Neumann et al., 1987). (Historical accounts of hurricanes prior to 187 1 back to the late 1700s are available from Ludlum (1963); the accuracy of these reports is excellent for near the coast but diminishes as the storms move inland.) For this study, we were interested in hurricanes that passed near the city of New Orleans, Louisiana. A review of hurricane paths since 1871 from Neumann et al. (1987) shows that

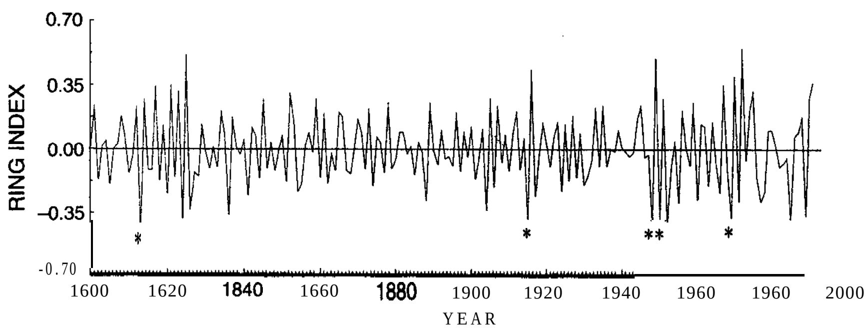

Figure 38.1. Standardized ring-width series from the Tangipahoa River basin. Large negative ring-width indices coincide with known hurricanes in 1812, 1915, 1947, 1948, and 1969.

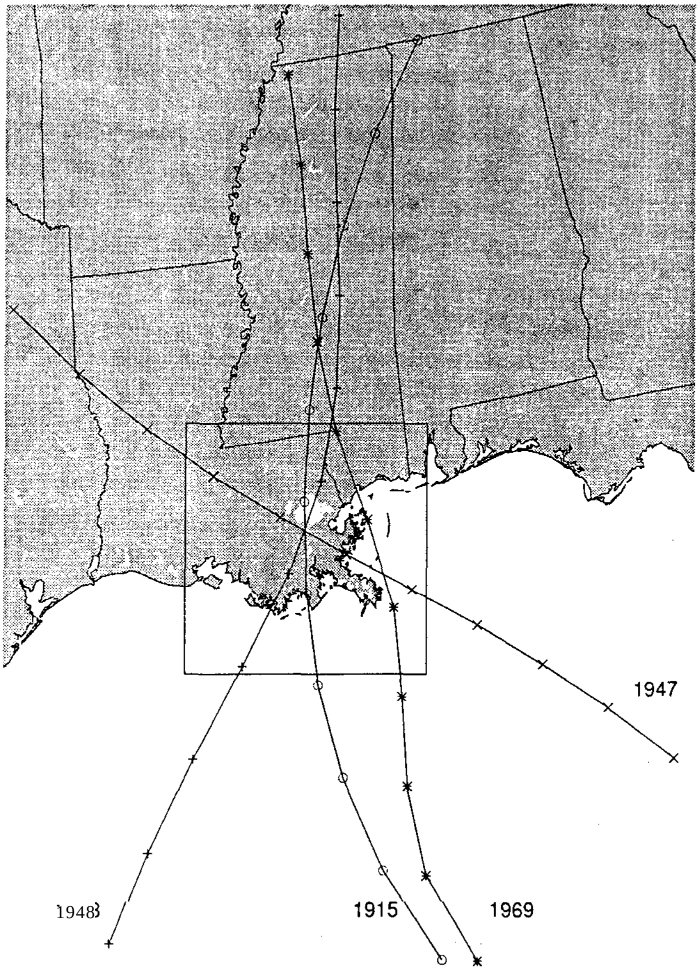

Figure 38.2. Paths of hurricanes in the vicinity of New Orleans and the Tangipahoa River and Pearl River study sites since 1915.

four hurricanes passed over New Orleans and the baldcypress forests in the Tangipahoa River study area (Figure 38.2).

In an attempt to evaluate the existence of a hurricane signal in baldcypress ring-width series we chose the following logic. We first developed a climate-tree-growth model using ordinary least squares (OLS), then looked at several regression diagnostics that provided information about influential data points and leverage points. If the regression diagnostics indicated that certain years had large residuals or leverage points, then we investigated whether these years were associated with known hurricane strikes. Prior studies have shown that standardized ring-widths of baldcypress are positively correlated with the PDSI for the month of June and spring precipitation on a wide regional basis (Stahle and Cleaveland, 1992), and we focused our efforts on investigating whether similar relationships existed for near-coastal baldcypress.

Ring widths from nineteen old-growth (> 400 years) baldcypress were measured, crossdated and then standardized using the inverse-hypersine transformation:

$$h(i) = \ln(r(i) + \sqrt{[r(i)^2 + 1]})$$

in which h is standardized ring-width, r is the actual ring-width and i is an index for years. First differences of the inverse-hypersines are nearly identical with first differences of natural logarithms, however, the transformation avoids the problem of a zero value for a ring-width returning a value of minus infinity (Van Deusen, 1990). We then developed OLS models using monthly average temperature, precipitation, and PDSI from 1895 to 1991, fit to the standardized ring-width data.

Regression Diagnostics

A valuable regression diagnostic statistic is the COVRATIO statistic, based on the ratio of the covariance matrix derived from all the data, $\sigma^2(X^TX)^{-1}$, with the covariance matrix that results when row i has been deleted, $\sigma^2[X^T(i)X(i)]^{-1}$ (Belsley et al., 1980). Because the two matrices differ only by the inclusion of the i'th row in the sum of squares and cross-products, values of this ratio near unity can be taken to indicate that the two covariance matrices are close, and the estimated coefficients are insensitive to deletion of the observation. Values farthest removed from unity indicate that the data for that specific year influence the estimated coefficients and therefore warrant further investigation.

Results and Discussion

Example Application of the Baysian Climate Reconstruction

We used cross-dated baldcypress tree-ring data from the Tangipahoa River basin just north of Lake Ponchartrain near New Orleans, Louisiana to reconstruct the PDSI for the month of June. June PDSI yields the highest R^2 value of any simple linear regression that regresses ring-widths on monthly temperature, precipitation, or PDSI with these data.

The following equation was used for calibrating the climate data to the tree-ring data:

$$f(y_t) = a + by_t \tag{2a}$$

in which the a and b parameters were estimated from that part of the data when both X and Y are known. Weighted regression was used with the weights being $1/\sigma_t^2$. The y_t chronology values were derived from taking first differences of natural logs for each core in the data set and then averaging. The q-parameter in equation (la) was estimated as follows:

$$q = \frac{\hat{e}'W\hat{e}}{n - 2} \tag{2b}$$

in which $\hat{e}$ is a vector of regression residuals, W is a diagonal matrix containing the weights and n is the number of known climate values.

The prior model for climate was an AR(2) model that was lit to the known PDSI values for the month of June.

$$g(X_{-t}) = \lambda_0 + \lambda_1 x_{t-1} + \lambda_2 x_{t-2} \tag{2c}$$

The A-parameters in (2c) are estimated from the known PDSI values using OLS and the p-parameter in equation (1 b) is the resulting mean squared error.

We initialized the Gibbs sampler with PDSI predictions from the calibration equation (2a). The usual practice for climate reconstruction would be to use these as the final values. Our approach calls for generating random variates distributed as N(0,1) and converting these to $N(\hat{x}_t, D^{-1})$ by sequentially stepping through the sequence called for by the Gibbs sampler. As mentioned earlier, convergence was assumed after 1,000 iterations, and 1,000 independent samples were generated at each step of the Gibbs sampler. The programming required here is trivial and allows us to easily compute valid confidence intervals.

The reconstruction was also performed over the period of known climate to indicate the Bayesian procedure's performance vs the traditional reconstruction from the calibration equation. In fact, there was only a slight improvement with the Bayes procedure (Figure 38.3); the sum of squared deviations for the Bayes procedure vs the squared deviations for the calibration equation differed by approximately 2% over the period of known climate. Model predictions from both the traditional and Bayesian procedure underpredict the (year-to-year) extreme observed values. This is an expected and well-known outcome when using OLS procedures for parameter estimation. The 95% prediction interval (CI) computed from the Gibbs sampler, although valid, is not very encouraging (Figure 38.4). The CI indicates that any value between about -2 and $+2$ is included at nearly all years. It is important to note that this CI is somewhat smaller that the CI that would be obtained with the usual calibration equation reconstruction. The prior information has kept the CI from being even larger.

Hurricane Signal

Similar to Stahle et al. (1988) and others, we found that the PDSI for the month of June was consistently the single-most influential variable. The regression model for coastal Louisiana that relates standardized tree growth as a function of climate is:

$$\hat{Y}_t = 0.003965 + 0.06067 \text{ (June PDSI}_t) \tag{3}$$

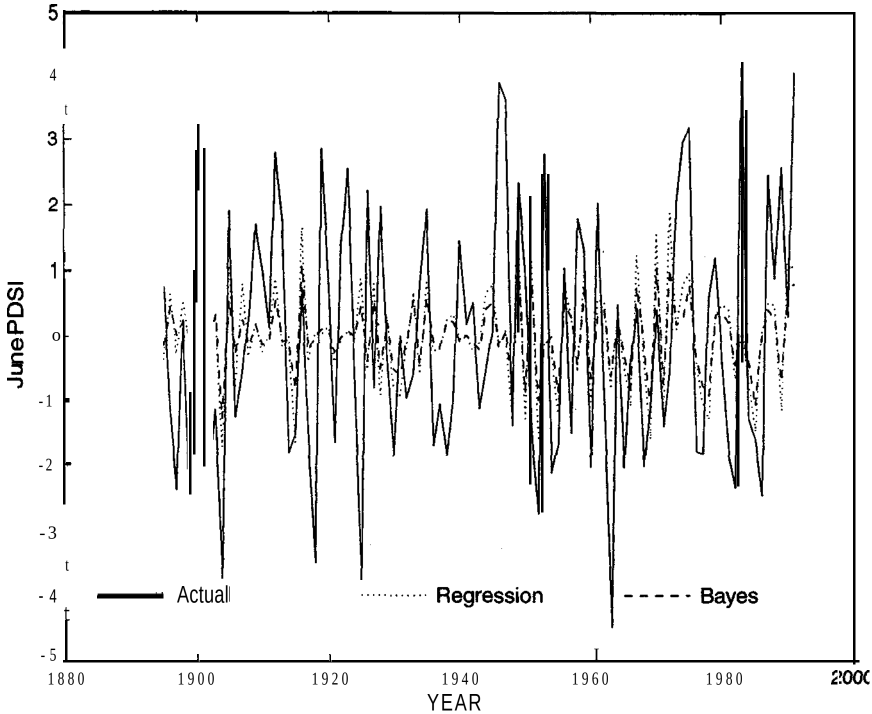

Figure 38.3. Reconstruction over the period of known PDSI for the month of June. The regression procedure results are represented by a dotted line, the Bayes results by a dashed line, and actual PDSI values by a solid line.

in which the subscript t is an index for year. Although the regression is significant at the $p < 0.003$ level, the model R^2 of. 10 is unimpressive. We suspect there are several reasons for the relatively weak performance of June PDSI found here as compared with other studies involving baldcypress. First, extended droughts along the coast of Louisiana are rarer than at sites farther inland, as summer afternoon thunderstorms are the norm even during regional inland droughts. The Louisiana (Division six) climate data illustrates the point that long runs of moisture deficits are not apparent in the data available from 1895 to 199 1 (Figure 38.5). Second, small ring-widths occur not only for drought years but also for the year of or after a hurricane. This probably causes a confounding of the drought signal and the hurricane signal. Such an interpretation suggests that the climate-growth relationship can change over time. Recent work in dendroecology has shown that climate-growth relationships can be dynamic and change for a number of reasons (Van Deusen, 1987; Peterson and Peterson, 1994).

Large swings between negative and positive studentized residuals occurred for years surrounding 1916, 1970, and during the late 1940s. All of these years followed known hurricane strikes (Figure 38.6). The COVRATIO residuals indicate that 1916, 1970, and the late 1940s are influential data points (Figure 38.7),

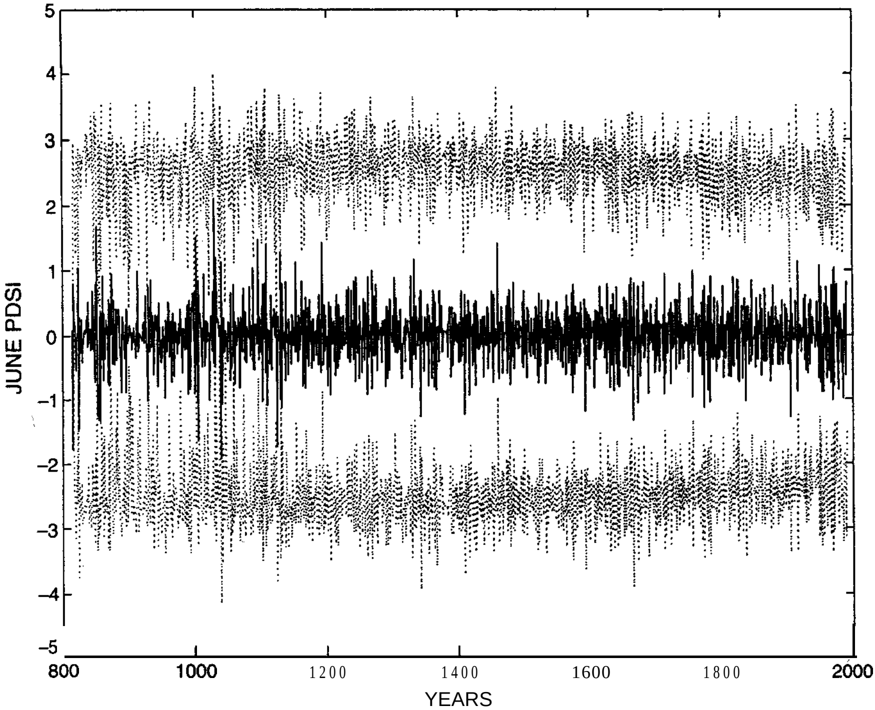

Figure 38.4. Reconstruction of June PDSI over the years 1814-1991 with 95% interval showing the range within which a reasonable climate prediction might fall for each year.

and all coincide with known hurricanes (Figure 38.2). Other such influential data points as 1905 and the mid-1950s appear to be associated with drought (negative PDSI values for June). From the two regression diagnostics, it appears that the most influential data points are associated with summer drought (noted in prior

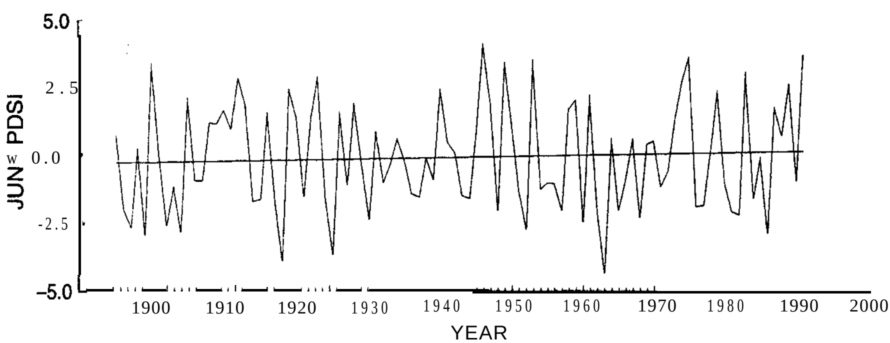

Figure 38.5. June PDSI from 1895-1991 for southeastern Louisiana. The trend line was estimated by fitting a first-degree orthogonal polynomial to the data.

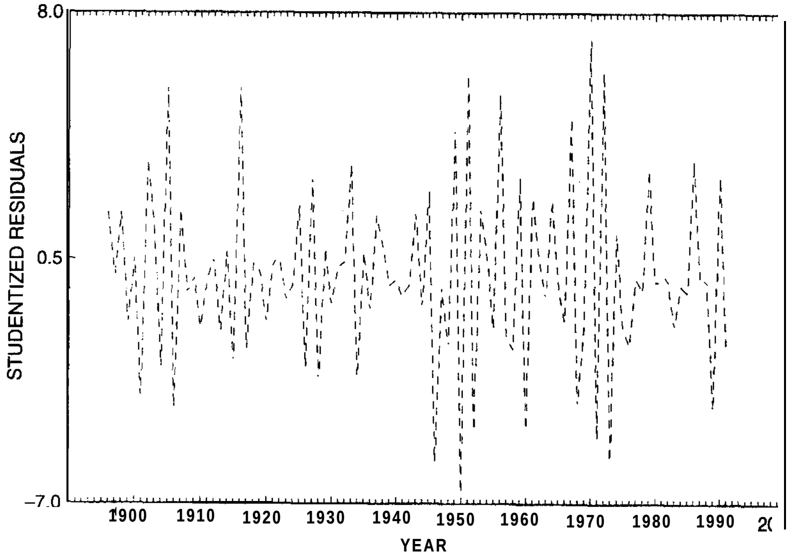

Figure 38.6. Studentized residuals from equation 1. Extreme residuals, both positive and negative, occur in the years that bound known hurricanes (1915, 1969, and the late 1940s)

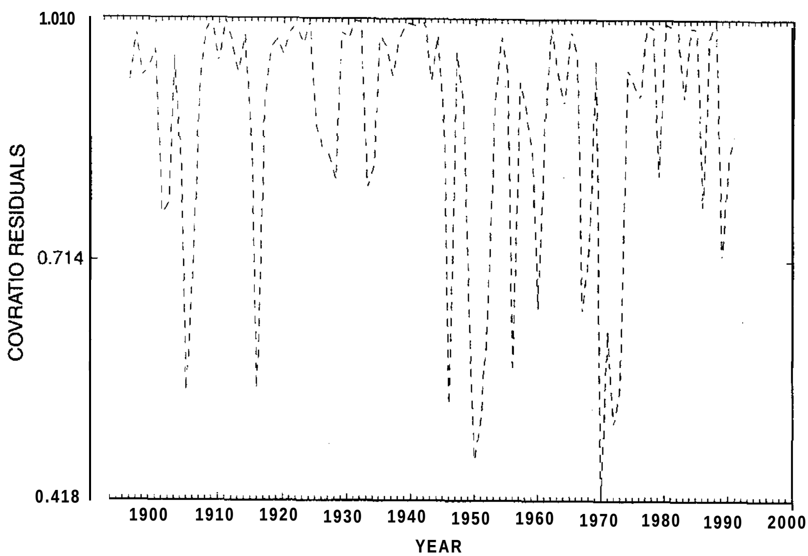

Figure 38.7. COVRATIO residuals from equation 1. Values farthest from unity are data points that heavily influence estimated coefficients. Residuals for the year 1916, 1970, and the late 1940s all coincide with known hurricanes.

baldcypress research) and hurricanes. Both phenomena result in small annual rings. Stahle and Cleaveland (1992) have presented evidence explaining the relationship between reduced ring-widths in baldcypress and drought. We suggest that the mechanism producing small ring-widths following a hurricane is foliage reduction through loss of small and large branches. Francis and Gillespie (1993) related maximum wind gust speeds during Hurricane Hugo to tree damage. They found that large trees were at greater risk than smaller trees, and that crown and bole damage began at speeds of about 60 km/hour (hr) and increased rapidly with gust speeds to about 130 km/hr. Our personal observations of baldcypress conditions in southern Louisiana following Hurricane Andrew in July and August of 1992 were similar to findings of Francis and Gillespie (1993) in that larger, older baldcypress lost individual large branches, while smaller, younger baldcypress appear to be relatively undamaged. Loope et al. (1994) also report that almost all old-growth baldcypress (> 300 years old) from the Corkscrew Swamp in southwest Florida lost upper portions of stems of major branches as a result of recent hurricanes (e.g., Andrew in 1992) and those in the past (Duever, et al., 1984). These observations appear to coincide with the lack of a clear hurricane signal in younger baldcypress when compared to old-growth cypress.

Late Spring and Summer Precipitation

Two approaches have been used by climatologists to derive scenario patterns of climatic changes that might result from an increase in atmospheric CO,. These are 1) numerical modelling using general circulation models (GCMs), and 2) the use of past warm periods as analogues of the future (Wigley et al., 1980). Both methods have limitations, however, it is noteworthy that there is agreement between the approaches on many of the general results. These results indicate that the greatest temperature changes will occur at high northern latitudes and in the winter.

For southern U.S. forests, regional changes in precipitation patterns are among the most important consequences of climatic warming, nevertheless there is substantial disagreement as to the magnitude and direction of changes. For example, in the lower southeastern United States, studies of the instrument-based climatic record have shown a correlation between increased temperature and increased annual precipitation (Diaz and Quayle, 1980). Conversely, Wigley et al., (1980) suggest that this region would be drier on an annual basis during a warm episode. A more recent analysis by Coleman (1988) suggests a decrease in summer convection activity that would result in reduced summer precipitation from 10 to 20%. Coleman (1988) concludes that deficits greater than these may occur under full-scale climatic warming.

The baldcypress chronologies are positively correlated with the PDSI for June and, therefore, decreases in productivity of baldcypress are probable under the decreased summer precipitation scenario (Wigley et al., 1980; Coleman, 1988). The bulk of rainfall in the lower southeastern United States during June, July, August, and September results from two distinct phenomena with climatically different origins, which are 1) convection thunderstorms, and 2) tropical cyclones. If the suggested decreases in summer precipitation occur from global warming we can expect decreased productivity for baldcypress, and possible reductions in baldcypress habitat because of drier soil conditions.

How this decreased summer precipitation will effect seed production and seedling development is not known. However, it is known that floodwaters spread the scales or cones along streams and this is the most important means of seed dissemination (USDA Forest Service, 1965). Seeds usually fail to germinate on better-drained soils as a result of reduced surface water. Thus, saturated soils are needed for a period of one to three months after seedfall. After germination, seedlings cannot endure submergence by flooding, therefore, provided there is success with germination, there are some possible benefits that could result from decreased summer precipitation.

Summary

The Bayesian reconstruction procedure presented here allows ‘for some prior knowledge about climate to be incorporated into the process. As specified earlier, the weight placed on the prior will tend to increase as the reconstruction moves further back in time. This is because the number of tree-ring observations diminishes and therefore σ_t^2 increases. It is not difficult to extend this approach to reconstruct a vector of climate values with a prior that accounts for intercorrelations among them. However, this extension is beyond the scope of this chapter.

Although the climate reconstruction in the example is somewhat disappointing, this reflects the inexact relationship between the tree-ring data and the climate data, and is not an indictment of the Bayes procedure. The Bayes procedure and the Gibbs sampler produce valid confidence intervals that are easy to produce.

For reconstructing variables other than PDSI, the climate data might need to be standardized to better meet the normal distribution assumption. The Palmer drought severity index by its nature is already standardized. There is clearly a need for further research on Bayesian climate reconstruction and the Gibbs sampler. We believe that the method will show particular promise for vector climate reconstruction because values within the same year have strong correlations that can be modeled with the prior distribution.

The use of the COVRATIO statistic for signal detection was successful in identifying both hurricane and drought events. The COVRATIO results indicate that the most influential data points affecting dendroclimatic parameter estimation are those years associated with hurricane strikes. From 1915 to 1991 there were four hurricanes that passed over the Tangipahoa River study site. Tree rings from old-growth baldcypress contain a hurricane signature that mimicked that of drought (reduced growth). Fortunately, the differences were apparent between drought and hurricane signals. We observed a notable increase in high frequency ring-width variation associated with hurricanes that does not appear around periods of drought. However, climate reconstructions based on tree-ring material from coastal areas with a relatively high frequency of hurricanes should take into account the possibility that depressed ring-widths from hurricanes might mimic those caused by drought.

Crown damage to old-growth trees seems the most probable mechanism by which passing hurricanes are recorded. Old-growth baldcypress from our study suffered from heavy crown damage and subsequent heartrot caused by a fungus that gained entry in the crown and worked downward over the centuries. To date, we have not detected a hurricane signal from second-growth baldcypress. Our observations following Hurricane Andrew in 1992 suggest that in addition to loss of needles, young baldcypress trees experience less crown damage than old-growth trees.

References

Baillie MGL, Munro MAR (1988) Irish tree rings, Santorini and volcanic dust veils. Nature 332:344–346.

Belsley DA, Kuh E, Welsch RE (1980) *Regression diagnostics: Identifying influential data and sources of collinearity* John Wiley and Sons, New York.

Box GEP, Tiao GC (1973) *Bayesian inference in statistical analysis.* Addison-Wesley, Philippines.

Carlin BP, Gelfand AE, Smith AFM (1992) Hierarchical Bayesian analysis of changepoint problems. Appl Stat 41(2):389–405.

Coleman JM (1988) Climatic warming and increased summer aridity in Florida, U.S.A. Clim Change 12:165–178.

Conner WH, Toliver JR (1990) Long-term trends in the bald-cypress (*Taxodium distichum*) resource in Louisiana (U.S.A.). For Ecol and Manage 33/34:543–557.

Diaz MF, Quayle RG (1980) The climate of the United States since 1895: Spatial and temporal changes. Mon Weat Rev 108:246–266.

Douglass AE (1941) Crossdating and dendrochronology. J For 39:825–831.

Duever MJ, Carlson JE, Riopelle LA (1984) Corkscrew Swamp: A virgin cypress stand. In Ewel KC, Odum T (Eds) *Cypress swamps.* University Presses of Florida, Gainesville, 334-348.

Emanuel KA (1987) The dependence of hurricane intensity on climate. Nature 326:483-485.

Francis JK, Gillespie AJR (1993) Relating gust speed to tree damage in Hurricane Hugo, 1989. J Arbor 19(6):368–373.

Fritts HC (1976) *Tree rings and climate.* Academic Press, London.

Geman S, Geman D (1984) Stochastic relaxation, Gibbs distributions, and the Bayesian restoration of images. IEEE Transactions on Pattern Analysis and Machine Intelligence, PAMI-6:721–741.

Graumlich LJ (1993) A 1000-year record of temperature and precipitation in the Sierra Nevada. Quat Res 39:249–255.

Graybill DA, Idso SB (1993) Detecting the aerial fertilization effect of atmospheric CO_2 enrichment in tree-ring chronologies. Glob Biogeochem Cyc 7:81–95.

Jarrell JD, Elsberry RL (1994) The effect of global climate change on tropical cyclones. Paper presented at the 5th Global Warming Conference, San Francisco, California. 4-7 April.

Loope L, Duever M, Herndon A, Snyder J, Jansen D (1994) Hurricane impacts on uplands and freshwater swamp forests. BioSci 44(4):238–246.

Ludlum DM (1963) *Early American hurricanes 1492–1870.* Lancaster Press, Inc, Boston.

Neumann CJ. Jarvinen BR, Pike AC, Elms JD (1987) Tropical Cyclones of the *North Atlantic* ocean, *1871–1986.* Historical Climatology Series 6-2. National Climatic Data Center, Asheville, NC.

Peterson, DW, Peterson DL (1994) Effects of climate on radial growth of subalpine conifers in the North Cascade Mountains. Can J For Res 24:1921–1932.

Putz FE, Sharitz RR (199 1) Hurricane damage to old-growth forest in Congaree Swamp National Monument, South Carolina, U.S.A. Can J For Res 21:1765–1770.

Reams GA, Van Deusen PC (1993) Synchronic large-scale disturbances and red spruce growth decline. Can J For Res 23:1361–1374.

Rosson JF, McWilliams WH, Frey PD (1988) Forest resources of Louisiana. USDA For Serv Resour Bull, SO-130.

Schmidt H, von Storch H (1993) German bight storms analyzed. Nature 365:791.

Sheffield RM, Thompson MT (1992) *Hurricane Hugo: Effects on South Carolina 's Forest Resource.* Research Paper SE-284. USDA, For Serv, Southeast For Exper Stat, Asheville, NC.

Sheppard PR, Jacoby GC (1987) Dating earthquakes along the San Andreas fault system in California. In Jacoby GC, Hombeck JW, (Eds) *Proceedings of the international symposium on ecological aspects of tree-ring analysis.* US Department of Commerce, Springfield, VA.

Smith AFM, Gelfand AE (1992) Bayesian statistics without tears: A sampling-resampling perspective. Amer Stat 46:84–88.

Stahle DW, Cook ER, White JWC (1985) Tree-ring dating of baldcypress and potential for millennia-long chronologies in the Southeast. Amer Anti 50:796–802.

Stahle DW, Cleaveland MK, Hehr JG (1988) North Carolina climate changes reconstructed from tree rings: A.D. 372 to 1985. Science 240:1517–1519.

Stahle DW, Cleaveland MK (1992) Reconstruction and analysis of spring rainfall over the southeastern U.S. for the past 1000 years. *Bull Amer Met Soc* 73(12): 1947-1961.

Stahle DW, Cleaveland MK (1993) Southern oscillation extremes reconstructed from tree rings of the Sierra Madre Occidental and Southern Great Plains. J Clim 6(1): 129-140.

Swetnam TW (1993) Fire history and climate change in giant sequoia groves. Science 262:885–889.

U.S. Department of Agriculture, Forest Service (1965) *Silvics of forest trees of the United States.* USDA, Agriculture Handbook 27 1. Washington, DC.

Van Deusen PC (1987) Testing for stand dynamics effects on red spruce growth trends. Can J For Res 17: 1487-1495.

Van Deusen PC (1990) A dynamic program for cross-dating tree rings. Can J For Res 20:200–205.

Wigley TML, Jones PD, Kelly PM (1980) Scenario for a warm, high-CO, world. Nature 283:17–21.

Wilhite LP, Toliver JR (1990) Taxodium distichum. In Bums RM, Honkala BH, (Eds) *Silvics of North America.* U.S. Department of Agriculture, Forest Service Agriculture Handbook 654. Washington, DC.

Williston HL, Shropshire FW, Balmer WE (1980) Cypress management: A forgotten opportunity. USDA For Rep SA-FR-8.